JACS
JOURNAL OF THE AMERICAN CHEMICAL SOCIETY

Communication

pubs.acs.org/JACS

Ultrasmall Near-Infrared Ag_2Se Quantum Dots with Tunable Fluorescence for *in Vivo* Imaging

Yi-Ping Gu,[†,§] Ran Cui,[†,§] Zhi-Ling Zhang,[†] Zhi-Xiong Xie,[‡] and Dai-Wen Pang*[,†]

[†]Key Laboratory of Analytical Chemistry for Biology and Medicine (Ministry of Education), College of Chemistry and Molecular Sciences, Research Center for Nanobiology and Nanomedicine (MOE 985 Innovative Platform), State Key Laboratory of Virology, and Wuhan Institute of Biotechnology, Wuhan University, Wuhan, 430072, P. R. China

[‡]College of Life Sciences, Wuhan University, Wuhan 430072, P. R. China

Supporting Information

ABSTRACT: A strategy is presented that involes coupling Na_2SeO_3 reduction with the binding of silver ions and alanine in a quasi-biosystem to obtain ultrasmall, near-infrared Ag_2Se quantum dots (QDs) with tunable fluorescence at 90 °C in aqueous solution. This strategy avoids high temperatures, high pressures, and organic solvents so that water-dispersible sub-3 nm Ag_2Se QDs can be directly obtained. The photoluminescence of the Ag_2Se QDs was size-dependent over a wavelength range from 700 to 820 nm, corresponding to sizes from 1.5 ± 0.4 to 2.4 ± 0.5 nm, with good monodispersity. The Ag_2Se QDs are less cytotoxic than other nanomaterials used for similar applications. Furthermore, the NIR fluorescence of the Ag_2Se QDs could penetrate through the abdominal cavity of a living nude mouse and could be detected on its back side, demonstrating the potential applications of these less toxic NIR Ag_2Se QDs in bioimaging.

Near-infrared (NIR) fluorescence facilitates bioimaging and biodetection because it involves less interference from blood and tissue autofluorescence and absorption.[1,2] Semiconductor nanocrystals (quantum dots, QDs) with fantastic optical properties, such as broad excitation, size-dependent photoluminescence, unusual photochemical stability, and single excitation/multiple emission, have attracted much attention in bioimaging. So far, only the following QDs are known to emit NIR fluorescence: (1) type-II nanomaterials of CdTe/CdSe core−shell;[3−5] (2) CdTeS, $CdTe_xSe_{1-x}$, and CdHgTe of alloy structure,[6−9] both types of which contain toxic heavy metals and are controversial for use in bioimaging and biodetection; and (3) some relatively environmentally friendly nanomaterials, including InAs/ZnSe,[10] InAs/InP,[11,12] InP/ZnS,[13,14] Ag_2S,[15] and Si QDs.[16]

Besides biocompatibility and nontoxicity, small size is also important for labeling nanomaterials. In general, existing QDs are close to or larger than most biological macromolecules in size. Thus, use of QDs in biological labeling may be limited due to their large size, which would interfere with both the recognition between QD-labeled bioprobes and target molecules due to steric hindrance and the movement of the bioprobes.[17] Therefore, it is still a big challenge to construct new fluorescent QDs with less toxicity and small size for bioimaging and biodetection.[17]

Ag_2Se nanocrystals are less toxic and less explored nanomaterials, usually found in two different stable solid phases: semiconducting β-Ag_2Se, synthesized at low temperature with an orthorhombic lattice and an energy gap of 0.07 eV at 0 K, and metallic α-Ag_2Se, synthesized at high temperature with a body-centered cubic lattice and superionic characteristics.[18a] Ag_2Se has been extensively studied in different fields over the past years.[18a,19−24] However, NIR optical applications of this environmentally friendly material[25] that does not involve heavy metals have been less investigated. Only the Heiss group has reported on two fluorescent wavelengths, 1030 and 1250 nm, of β-Ag_2Se QDs synthesized in the organic phase,[25] which need to be transferred to the aqueous phase for bioimaging. In order to avoid additional water solubilization, synthesizing nanocrystals in aqueous phase is a direct strategy to obtain water-dispersible nanocrystals for bioapplications. However, since the fluorescence is mainly controlled by the size of Ag_2Se nanoparticles[25] and Ag_2Se nanoparticles with small sizes are usually difficult to obtain in the aqueous phase,[18a] no report on fluorescence-tunable Ag_2Se nanoparticles synthesized in the aqueous phase has appeared so far.

Biochemical reactions and biosystems are powerful tools for controllable synthesis of nanomaterials.[26−28] Using a quasi-biosystem, 1.3 nm Au clusters have been successfully synthesized.[28] Herein, we report a strategy to synthesize NIR fluorescence-tunable, small size (sub-3 nm), and water-dispersible Ag_2Se QDs at 90 °C by mimetic biochemical reactions. The fluorescence properties, cytotoxicity, and potential ability for *in vivo* imaging using the as-prepared Ag_2Se QDs are demonstrated in this work.

The crucial point in preparing the Ag_2Se QDs is to obtain Ag and Se elements in the appropriate valence states. In previous reports, selenite was reduced to low-valence selenium in yeast cells,[29,30] which can react with Cd^{2+} to form fluorescent CdSe QDs in living yeast cells.[26] This process of selenite reduction from SeO_3^{2-} to GSSeH was biomimicked, using glutathione (GSH), reduced nicotinamide adenine dinucleotide phosphate (NADPH), and glutathione reductase (GR) as described in Figure 1. GSSeH, which can react with heavy metal ions,[31] was predesigned as the Se precursor for the synthesis of Ag_2Se QDs.

The reduction of SeO_3^{2-} with GSH was biomimicked to obtain GSSeSG by mixing 20 μL of 0.1 M Na_2SeO_3, 2.1 mL of

Received: September 23, 2011
Published: December 8, 2011

dx.doi.org/10.1021/ja2089553 | J. Am. Chem.Soc. 2012, 134, 79−82

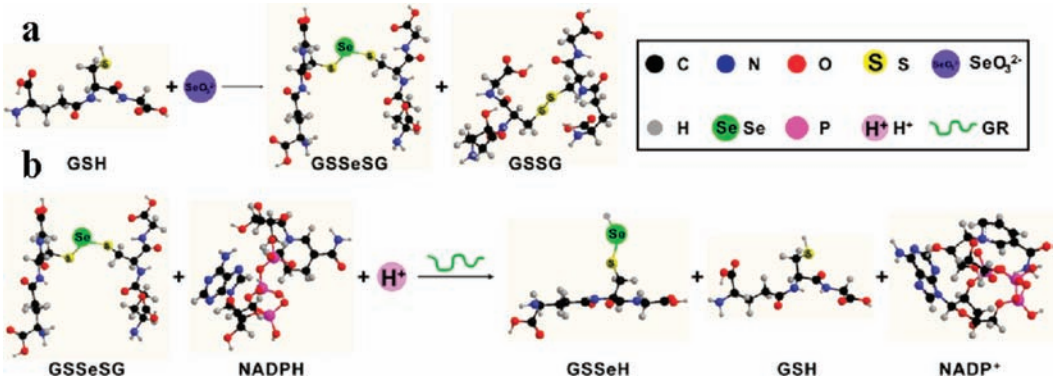

Figure 1. Scheme for SeO_3^{2-} reducing process including (a) reduction of SeO_3^{2-} with GSH and (b) reduction of GSSeSG with NADPH and GR.

pH 7.1 Britton–Robison (BR) buffer, and 80 μL of 0.1 M GSH and subsequently incubating for 1 min as previously reported.[29] High-performance liquid chromatography coupled with mass spectrometry (HPLC-MS) was used to monitor the designed process of selenite reduction. GSSeSG obtained from the reduction of Na_2SeO_3 by GSH in the first step of the reduction (Figure 1a) is the key intermediate for the formation of desired GSSeH. As confirmed by our HPLC results, there were three organic components in the first reduction step (Figure S1a). Mass spectra demonstrated that the three organic components were GSH, GSSG, and GSSeSG (Figure S1b–d). The hypothesized Se precursor (GSSeH) was also detected by HPLC-MS. The mass spectrum (Figure S2b) confirmed that the sample peak (41.97 min) in the HPLC chromatogram (Figure S2a) represented GSSeH, indicating that the GSSeH existed in the biomimetic process of selenite reduction. Hence, the desired Se precursor GSSeH could be indeed obtained according to our design.

Besides the Se precursor, an appropriate form of Ag precursor is important in order to prepare the monodispersed Ag_2Se QDs. Alanine (Ala), which can form a Ag^+-Ala complex,[32] was chosen as the stabilizer for Ag_2Se QDs. Therefore, we designed a strategy of coupling two biochemical processes, Na_2SeO_3 reduction and binding of silver ions and alanine, to construct a quasi-biosystem to realize the synthesis of Ag_2Se QDs in aqueous phase.

The freshly prepared Se precursors were injected into the solution of the fresh Ag^+-Ala precursors, and the mixture was stirred for 10 min at 90 °C, giving Ag_2Se QDs. All the characteristic peaks in the XRD results (Figure 2b) matched exactly with the standard JCPDS card (no. 24-1041).[19] This result suggested that the purified products synthesized by our method at 90 °C were orthorhombic Ag_2Se in the β form. The high-resolution transmission electron microscopy (HRTEM) image in Figure 2a shows that the lattice spacing (ca. 0.24 and 0.23 nm) agrees with the distances between adjacent facets (013) and (031) of orthorhombic Ag_2Se. Energy-dispersive X-ray spectroscopy (EDX) characterization (Figure S3) of the purified products proved that the products were composed of Ag and Se elements. X-ray photoelectron spectroscopy (XPS) was used to analyze the surface composition of the as-prepared products. The survey-scan and narrow-scan spectra of the Ag 3d and Se 3d are shown in Figure S4. The binding energy XPS data were referenced to the C 1s of aliphatic carbon at 284.9 eV. The peaks at 367.56 and 373.59 eV correspond to Ag $3d_{5/2}$ and $3d_{3/2}$, and the peak at 53.53 eV corresponds to Se 3d of Ag_2Se QDs. The binding energy obtained from XPS analysis is

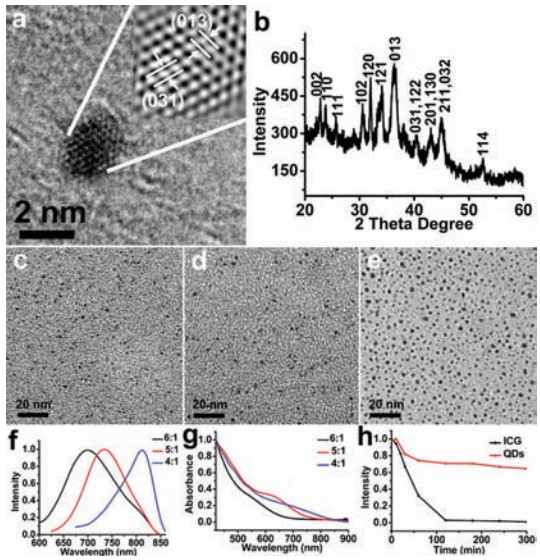

Figure 2. (a) HRTEM image, (b) XRD pattern, (c–e) TEM images of monodispersed Ag_2Se QDs with different sizes (synthesized at a 6:1 (c), 5:1 (d), and 4:1 (e) molar ratio of Ag precursor to Se precursor), (f) PL emission spectra, (g) absorption spectra, and (h) photostability curve of Ag_2Se QDs.

consistent with a previous report.[18a] The above results indicate that the products prepared by mimicking biochemical reactions were indeed orthorhombic Ag_2Se QDs.

Tuning the photoluminescence of NIR nanomaterials for biolabeling is still a big challenge. Since the optical properties of Ag_2Se QDs are size-dependent,[25] size control is crucial for tuning the photoluminescence wavelength. However, it is difficult to obtain Ag_2Se QDs with small size due to the small solubility product constant ($K_{SP} = 2.0 \times 10^{-64}$) of the Ag_2Se[18b] and the fast crystal growth.[18a] Hence, the NIR properties of this environmentally friendly material without heavy metals are not much investigated. Using this quasi-biosystem, ultrasmall Ag_2Se QDs can be obtained with varying sizes by changing the initial Ag:Se molar ratio. The sizes were obtained by measuring at least 300 individual Ag_2Se QDs in transmission electron microscopy (TEM) images. As shown in Figure 2c–e, by tuning the molar ratio of Ag precursor to Se precursor (6:1, 5:1, 4:1), uniform sub-3 nm Ag_2Se QDs can be synthesized with varying sizes of 1.5 ± 0.4, 1.6 ± 0.4, and 2.4 ± 0.5 nm, respectively. As the Ag:Se molar ratio decreased from 6:1 to 5:1 and to 4:1, the PL emission peak of the Ag_2Se QDs gradually shifted from 700 to 730 nm and to 820 nm (Figure 2f) with

dx.doi.org/10.1021/ja2089553 | J. Am. Chem.Soc. 2012, 134, 79–82

quantum yields 1.00%, 1.01%, and 3.09%, respectively, and the absorption peaks of the products in the UV−vis spectra (Figure 2g) red-shifted. It is worth noting that the full width at half-maximum (fwhm) of the PL emission peak (90−120 nm) of as-prepared Ag_2Se QDs is obviously narrower than those of the previously reported HgTe QDs,[33a] CdHgTe QDs,[33b] and Ag_2Se QDs[25] (about 200 nm).

The photostability of the as-prepared Ag_2Se QDs was characterized by continuous irradiation by an Hg lamp with a power of 50 W (Figure 2h). A widely used NIR organic dye, indocyanine green (ICG), was chosen as the control for the Ag_2Se QDs. The ICG was completely photobleached after 120 min of continuous irradiation, whereas Ag_2Se QDs retained 65% of its fluorescence after 300 min of continuous irradiation (Figure 2h). These results indicate that the as-prepared Ag_2Se QDs have good photostability.

Ag_2X (X = S, Se, Te) QDs without heavy metals are considered as more environmentally benign alternatives for infrared-active nanocrystal materials.[25] However, the toxicity of this kind of QDs has not been studied. Thereby, 3-[4,5-dimethylthiazol-2-yl]-2,5-diphenyltetrazolium bromide (MTT) assay, a standard cell viability assay, was used to test the cytotoxicity of the as-prepared Ag_2Se QDs. MTT is a water-soluble tetrazolium salt and can be converted to an insoluble purple formazan by succinate dehydrogenase in the mitochondria of living cells, while dead cells cannot convert the MTT. MDCK cells (normal kidney cells of a cocker spaniel), Vero cells (normal kidney cells of an African green monkey), and A549 cells (lung carcinoma cells) were exposed to Ag_2Se QDs at different concentrations from 0 to 47.4 μg/mL to test the influence of Ag_2Se QDs on cell viability. As shown in Figure 3a,

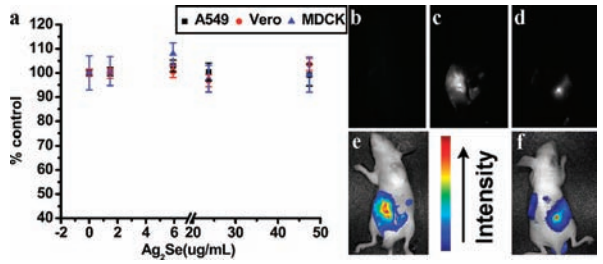

Figure 3. MTT assay and NIR images of a living nude mouse after injection of Ag_2Se QDs: (a) MTT assay on A549, Vero, and MDCK cells exposed to Ag_2Se QDs at different concentrations from 0 to 47.4 μg/mL for 24 h; (b) fluorescence image of the nude mouse; (c) fluorescence imaging from the abdominal cavity of the nude mouse with Ag_2Se QDs injected into the abdominal cavity; (d) fluorescence imaging on the back side of the nude mouse with Ag_2Se QDs injected into the abdominal cavity; (e,f) merged images of the bright-field and the threshold false color of (c) and (d), respectively.

97% of MDCK cells, 96% of Vero cells, and 100% of A549 cells retained viability after being exposed to the Ag_2Se QDs for 24 h. These results imply that the Ag_2Se QDs are relatively less cytotoxic and more environmentally friendly NIR nanomaterials.

The NIR fluorescence penetrability of the as-prepared Ag_2Se QDs *in vivo* was also demonstrated. The Ag_2Se QDs prepared by the above method are water-dispersible and thus can be used in biosystems without phase transfer from organic to aqueous phase. Ag_2Se QDs with PL emission at 820 nm were chosen for the living nude mouse imagin: 100 μL of Ag_2Se QDs in PBS buffer (1.5 mg/mL) were injected into the abdominal cavity of a mouse (~16 g) anesthetized with diethyl ether. As shown in Figure 3b−f, the NIR images could be obtained on the back side of the mouse after injection of Ag_2Se QDs into the abdominal cavity. The thickness of the mouse body was 2 cm, and the penetration depth of the as-prepared Ag_2Se QDs was at least 1 cm. The background spectrum of a nude mouse and the fluorescence spectrum of Ag_2Se QDs *in vivo* are shown in Figure S5. The fluorescence wavelengths from the nude mouse with and without Ag_2Se QDs were separated by about 80 nm. Furthermore, autofluorescence of the nude mouse was hardly observed, as shown in Figure 3b, thereby not influencing the *in vivo* imaging with Ag_2Se QDs. It should be emphasized that Ag_2Se QDs with >1% quantum yield can be used for NIR imaging. These results show that the NIR Ag_2Se QDs synthesized by coupling Na_2SeO_3 reduction with the binding of silver ions and alanine implies a promising future for their application of bioimaging.

In summary, we have coupled Na_2SeO_3 reduction with the binding of silver ions and alanine to successfully realize the synthesis of NIR fluorescence-tunable, small-size (sub-3 nm), less cytotoxic, and water-dispersible Ag_2Se QDs at 90 °C. By tuning the molar ratio of Ag precursor to Se precursor, sub-3 nm Ag_2Se QDs of varying sizes can be synthesized. The PL emission peak of Ag_2Se QDs has been tuned from 700 to 730 nm and to 820 nm, corresponding to sizes from 1.5 ± 0.4 to 1.6 ± 0.4 nm and to 2.4 ± 0.5 nm with quantum yields above 1%. The NIR fluorescence of the as-prepared Ag_2Se QDs can penetrate through a living nude mouse. Ag_2Se QDs may have promising applications in bioimaging.

■ ASSOCIATED CONTENT

Ⓢ Supporting Information

Details on the synthesis and characterization of Ag_2Se QDs, cell cultures and treatments, MTT assay, and imaging of living nude mice with Ag_2Se QDs. This material is available free of charge via the Internet at http://pubs.acs.org.

■ AUTHOR INFORMATION

Corresponding Author

dwpang@whu.edu.cn

Author Contributions

[§]These authors contributed equally to this work.

■ ACKNOWLEDGMENTS

This work was supported by the National Basic Research Program of China (973 Program, No. 2011CB933600), the Science Fund for Creative Research Groups of NSFC (No. 20921062), the National Natural Science Foundation of China (20833006; 21005056), and the "3551 Talent Program" of the Administrative Committee of East Lake Hi-Tech Development Zone ([2011]137).

■ REFERENCES

(1) Kim, S.; Lim, Y. T.; Soltesz, E. G.; Grand, A. M. D.; Lee, J.; Nakayama, A.; Parker, J. A.; Mihaljevic, T.; Laurence, R. G.; Dor, D. M.; Cohn, L. H.; Bawendi, M. G.; Frangioni, J. V. *Nat. Biotechnol.* **2004**, *22*, 93−97.

(2) Michalet, X.; Pinaud, F. F.; Bentolila, L. A.; Tsay, J. M.; Doose, S.; Li, J. J.; Sundaresan, G.; Wu, A. M.; Gambhir, S. S.; Weiss, S. *Science* **2005**, *307*, 538−544.

(3) Kim, S.; Fisher, B.; Eisler, H.-J.; Bawendi, M. *J. Am. Chem. Soc.* **2003**, *125*, 11466−11467.

(4) Seo, H.; Kim, S.-W. *Chem. Mater.* **2007**, *19*, 2715−2717.

(5) Yu, K.; Zaman, B.; Romanova, S.; Wang, D.-s.; Ripmeester, J. A. *Small* **2005**, *1*, 332−338.
(6) Qian, H.; Dong, C.; Peng, J.; Qiu, X.; Xu, Y.; Ren, J. *J. Phys. Chem. C* **2007**, *111*, 16852−16857.
(7) Bailey, R. E.; Nie, S. *J. Am. Chem. Soc.* **2003**, *125*, 7100−7106.
(8) Jiang, W.; Singhal, A.; Zheng, J.; Wang, C.; Chan, W. C. W. *Chem. Mater.* **2006**, *18*, 4845−4854.
(9) Mao, W.; Guo, J.; Yang, W.; Wang, C.; He, J.; Chen, J. *Nanotechnology* **2007**, *18*, 485611.
(10) Zimmer, J. P.; Kim, S.-W.; Ohnishi, S.; Tanaka, E.; Frangioni, J. V.; Bawendi, M. G. *J. Am. Chem. Soc.* **2006**, *128*, 2526−2527.
(11) Cao, Y. W.; Banin, U. *J. Am. Chem. Soc.* **2000**, *122*, 9692−9702.
(12) Cao, Y.-W.; Banin, U. *Angew. Chem., Int. Ed.* **1999**, *38*, 3692−3694.
(13) Haubold, S.; Haase, M.; Kornowski, A.; Weller, H. *Chemphyschem* **2001**, *5*, 331−334.
(14) Xie, R.; Battaglia, D.; Peng, X. *J. Am. Chem. Soc.* **2007**, *129*, 15432−15433.
(15) (a) Du, Y.; Xu, B.; Fu, T.; Cai, M.; Li, F.; Zhang, Y.; Wang, Q. *J. Am. Chem. Soc.* **2010**, *132*, 1470−1471. (b) Shen, S.; Zhang, Y.; Peng, L.; Du, Y.; Wang, Q. *Angew. Chem., Int. Ed.* **2011**, *50*, 7115−7118.
(16) (a) Mangolini, L.; Jurbergs, D.; Rogojina, E.; Kortshagen, U. *Phys. Stat. Sol. (c)* **2006**, *3*, 3975−3978. (b) Erogbogbo, F.; Yong, K.-T.; Roy, I.; Hu, R.; Law, W.-C.; Zhao, W.; Ding, H.; Wu, F.; Kumar, R.; Swihart, M. T.; Prasad, P. N. *ACS Nano* **2011**, *5*, 413−423.
(17) (a) Smith, A. M.; Duan, H.; Mohs, A. M.; Nie, S. *Adv. Drug Delivery Rev.* **2008**, *60*, 1226−1240. (b) Smith, A. M.; Nie, S. *Nat. Biotechnol.* **2009**, *27*, 732−733.
(18) (a) Ge, J.-P.; Xu, S.; Liu, L.-P.; Li, Y.-D. *Chem.—Eur. J.* **2006**, *12*, 3672−3677. (b) Wang, X.; Peng, Q.; Li, Y.-D. *Acc. Chem. Res.* **2007**, *40*, 635−643.
(19) Wang, D.; Xie, T.; Peng, Q.; Li, Y. *J. Am. Chem. Soc.* **2008**, *130*, 4016−4022.
(20) Ng, M. T.; Boothroyd, C.; Vittal, J. J. *Chem. Commun.* **2005**, 3820−3822.
(21) Cao, H.; Xiao, Y.; Lu, Y.; Yin, J.; Li, B.; Wu, S.; Wu, X. *Nano Res.* **2010**, *3*, 863−873.
(22) Cui, Y.; Chen, G.; Ren, J.; Shao, M.; Xie, Y.; Qian, Y. *J. Solid State Chem.* **2003**, *172*, 17−21.
(23) Liu, H.; Zhang, B.; Shi, H.; Tang, Y.; Jiao, K.; Fu, X. *J. Mater. Chem.* **2008**, *18*, 2573−2580.
(24) Sahu, A.; Qi, L.; Kang, M. S.; Deng, D.; Norris, D. J. *J. Am. Chem. Soc.* **2011**, *133*, 6509−6512.
(25) Yarema, M.; Pichler, S.; Sytnyk, M.; Seyrkammer, R.; Lechner, R. T.; Fritz-Popovski, G.; Jarzab, D.; Szendrei, K.; Resel, R.; Korovyanko, O.; Loi, M. A.; Paris, O.; Hesser, G.; Heiss, W. *ACS Nano* **2011**, *5*, 3758−3765.
(26) Cui, R.; Liu, H.-H.; Xie, H.-Y.; Zhang, Z.-L.; Yang, Y.-R.; Pang, D.-W.; Xie, Z.-X.; Chen, B.-B.; Hu, B.; Shen, P. *Adv. Funct. Mater.* **2009**, *19*, 2359−2364.
(27) (a) Cui, R.; Zhang, M.-X.; Tian, Z.-Q.; Zhang, Z.-L.; Pang, D.-W. *Nanoscale* **2010**, *2*, 2120−2125. (b) Zhang, M.-X.; Cui, R.; Zhao, J.-Y.; Zhang, Z.-L.; Pang, D.-W. *J. Mater. Chem.* **2011**, *21*, 17080−17082.
(28) Zhang, M.-X.; Cui, R.; Tian, Z.-Q.; Zhang, Z.-L.; Pang, D.-W. *Adv. Funct. Mater.* **2010**, *20*, 3673−3677.
(29) Kessi, J.; Hanselmann, K. W. *J. Biol. Chem.* **2004**, *279*, 50662−50669.
(30) Ganther, H. E. *Biochemistry.* **1971**, *10*, 4089−4098.
(31) Reddy, C. C.; Massaro, E. J. *Fund. Appl. Toxicol.* **1983**, *3*, 431−436.
(32) Shoeib, T.; Siu, K. W. M.; Hopkinson, A. C. *J. Phys. Chem. A* **2002**, *106*, 6121−6128.
(33) (a) Kovalenko, M. V.; Kaufmann, E.; Pachinger, D.; Roither, J.; Huber, M.; Stangl, J.; Hesser, G.; Schäffler, F.; Heiss, W. *J. Am. Chem. Soc.* **2006**, *128*, 3516−3517. (b) Rogach, A. L.; Harrison, M. T.; Kershaw, S. V.; Kornowski, A.; Burt, M. G.; Eychmüller, A.; Weller, H. *Phys. Stat. Sol. (b)* **2001**, *224*, 153−158.